

# Superconductivity in $\text{La}T_M\text{BN}$ and $\text{La}_3T_{M2}\text{B}_2\text{N}_3$ ( $T_M = \text{Transition Metal}$ ) Synthesized under High Pressure

Naoki Imamura,<sup>†</sup> Hiroshi Mizoguchi,<sup>†</sup> and Hideo Hosono<sup>\*,†,‡</sup>

<sup>†</sup>Frontier Research Center, and <sup>‡</sup>Materials and Structures Laboratory, Tokyo Institute of Technology, Yokohama 226-8503, Japan

**S** Supporting Information

**ABSTRACT:** Various layered boronitrides  $(\text{LaN})_n(T_{M2}\text{B}_2)$  ( $T_M = \text{transition metal}$ ;  $n = 2, 3$ ) have been prepared using a high-pressure synthesis technique in which an inverse  $\alpha\text{-PbO}$ -type  $T_{M2}\text{B}_2$  layer is separated by two or three rock salt-type  $\text{LaN}$  layers and these layers are connected through linear (BN) units. The electronic states of the distinguishing (BN) unit and intermediate rock salt-type  $\text{LaN}$  layer are discussed on the basis of density functional theory calculations. Bulk superconductivity has been found in  $\text{LaNiBN}$  ( $T_c \approx 4.1$  K),  $\text{CaNiBN}$  ( $T_c \approx 2.2$  K), and  $\text{LaPtBN}$  ( $T_c \approx 6.7$  K), where the Fermi level  $E_F$  is located in the bands composed of the  $T_M(\text{d})\text{-B}(2\text{p})$  antibonding state and the main  $T_M(\text{d})$  band resides well below  $E_F$ . The non-superconductive  $T_M$ -based compounds exhibit Pauli paramagnetic behavior, in which the highly itinerant nature of the electrons caused by strong  $T_M(\text{d})\text{-B}(2\text{p})$  covalent bonding suppresses the long-range magnetic ordering.

The discovery of superconductivity in  $\text{LaFeAs}(\text{O},\text{F})$  has directed considerable attention to compounds containing tetrahedrally coordinated square nets of  $\text{Fe}^{2+}$ .<sup>1</sup> The exploration of unconventional superconductors, such as Fe-based pnictides with superconducting transition temperatures ( $T_c$ ) that lie next to those of copper oxide superconductors,<sup>1</sup> is a challenge from both fundamental and technological points of view. There is a rich variety of transition metal ( $T_M$ )-based compounds containing the structural unit of a square lattice of  $T_M$  elements with tetrahedral coordination that is similar to the Fe-based superconductors. New superconductors have been found among these materials, indicating that such a structural unit can be a platform for superconductivity. The Ni-based intermetallic compounds  $\text{RNi}_2\text{B}_2\text{C}$  ( $R = \text{rare-earth element}$ ), which consist of alternative stacking of an inverse  $\alpha\text{-PbO}$ -type  $\text{Ni}_2\text{B}_2$  layer and a rock salt (RS)-type  $\text{RC}$  layer, have been widely studied because of their relatively high  $T_c$  values and the intriguing competitive relationship between superconductivity and magnetism in some magnetic  $R$  series.<sup>2</sup>

From a structural point of view, the inverse  $\alpha\text{-PbO}$ -type layer consisting of a  $T_M$  square net and a boron ligand is atypical because the rigid (BC), (BN), or (BCB) structural unit is usually present perpendicular to the  $T_M$  sheet in borocarbides and -nitrides. The above-mentioned  $\text{RNi}_2\text{B}_2\text{C}$  belongs to the  $n = 1$  phase of the homologous series of  $(\text{RX})_n(\text{Ni}_2\text{B}_2)$  ( $X = \text{C}, \text{N}$ ;  $n = \text{integer}$ ) (see Figure 1). In the  $(\text{RX})_n(\text{Ni}_2\text{B}_2)$  series, the  $\text{Ni}_2\text{B}_2$  layers are separated by several RS-type  $\text{RX}$  layers ( $n$ ), and

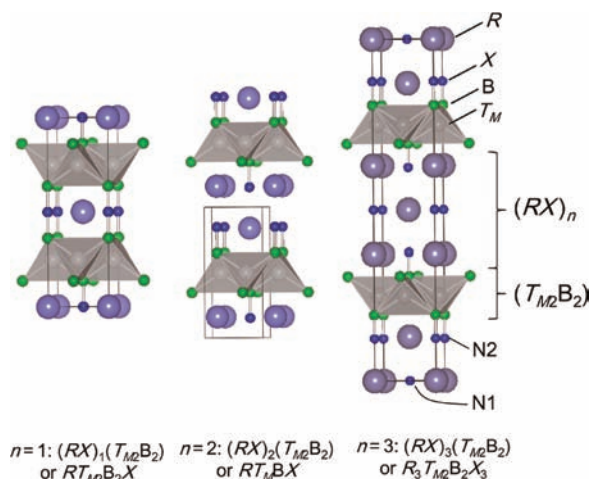


**Figure 1.** Crystal structures of the  $(\text{RX})_n(\text{T}_{M2}\text{B}_2)$  ( $R = \text{rare-earth element}$ ;  $X = \text{C}, \text{N}$ ;  $n = 1, 2, 3$ ) homologous series.

the inverse  $\alpha\text{-PbO}$ - and RS-type layers are connected through linear (BC), (BN), or (BCB) structural units. Until now, various superconductive borocarbides ( $n = 1, 2$ ) have been discovered, while only  $\text{La}_3\text{Ni}_2\text{B}_2\text{N}_3$  of the  $n = 3$  phase has been reported as a superconductive boronitride.<sup>3</sup> Despite the highly anisotropic two-dimensional (2D) crystal structure, a more 3D-like electronic structure was reported in  $(\text{RX})_n(\text{Ni}_2\text{B}_2)$ , where  $R$  is not fully ionized and the  $\text{RX}$  layer is metallic.<sup>4</sup>

$\text{RNi}_2\text{B}_2\text{C}$  and relevant  $\text{ThCr}_2\text{Si}_2$ -type pnictides  $\text{ANi}_2\text{Pn}_2$  ( $A = \text{alkaline-earth element}$ ;  $\text{Pn} = \text{pnictogen}$ ) have similar electronic structures, and the former possess higher  $T_c$ .<sup>4,5</sup> These experimental and theoretical studies on the Ni-based system together with discovery of high- $T_c$  Fe-based pnictides motivated us to explore various  $\text{T}_{M2}\text{B}_2$ -based compounds as candidates for high- $T_c$  superconductors. In contrast to the intensive study of borocarbides, including (BC) or (BCB) structural units, few boronitrides have been synthesized. This is because boronitrides are more difficult to synthesize than the corresponding borocarbides. N-for-C substitution in the  $\text{T}_{M2}\text{B}_2$ -based system would be expected to affect not only the physical properties influenced by electron doping but also its structural stability. Here we report the successful synthesis of new boronitrides with  $n = 2$  and 3 under high pressure along with studies of their electromagnetic properties, including superconductivity.

Received: December 2, 2011

Published: January 24, 2012

In addition to conventional solid-state reactions, various synthetic techniques have been developed to stabilize layered boronitrides  $(RN)_n(T_{M2}B_2)$ : (1) arc-melting under an  $N_2$  atmosphere,<sup>3</sup> (2) pyrolysis of a polymeric precursor,<sup>6</sup> and (3) solid-state metathesis reactions using the formation of  $LiCl$ .<sup>6</sup> In the present study, a high-pressure synthesis was employed to obtain highly crystalline and N-stoichiometric bulk samples. Both of these factors significantly affect the  $T_c$  of  $La_3Ni_2B_2N_3$ .<sup>6,7</sup> The starting materials used to synthesize  $(RN)_n(T_{M2}B_2)$  were  $LaN$ ,  $T_M$  and B powders. The transition metals examined in the present study are listed in Table S1 in the Supporting Information (SI), where the resultant phases are also shown. The starting materials were mixed well and loaded in a Ta capsule in an Ar-filled drybox. The Ta container was then welded inside the drybox to prevent degradation of the air-sensitive nitrides during synthesis and heat-treated at 2–5 GPa and 1200–1600 °C for 0.5–2 h (for details, see Table S1) using a belt-type high-pressure apparatus. For instance,  $LaNiBN$  was prepared at 5 GPa and 1200 °C for 0.5 h, and  $LaPtBN$  and  $CaNiBN$  were formed at 5 GPa and 1400 °C for 1 h.

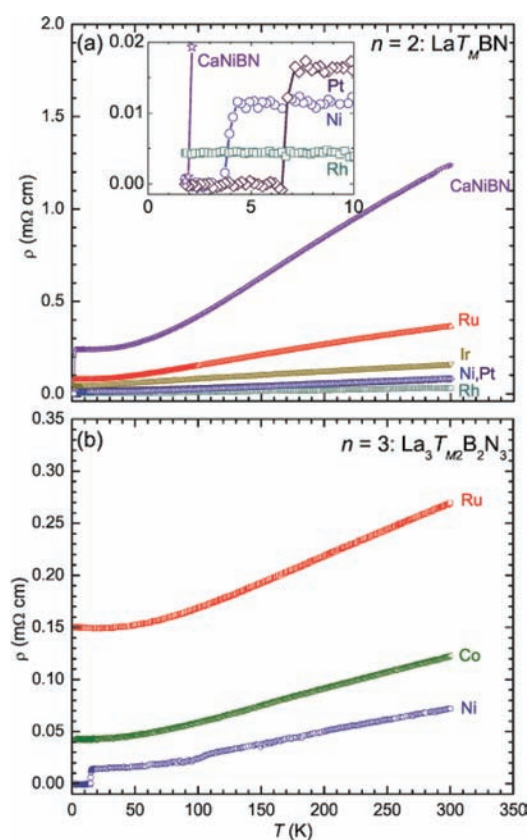
In the case of  $T_M = Ni$  and  $Ru$ , the  $n = 2$  and 3 phases often coexist when stoichiometric mixtures are used as starting materials. Therefore, the nominal chemical composition deviated from the ideal stoichiometry to reduce these competing phases. In particular,  $LaNiBN$  was prepared from a mixture of the raw materials with the nominal atomic ratio  $LaN:Ni:B = 0.9:1:1$ , while  $LaRuBN$  ( $n = 2$ ) and  $La_3Ru_2B_2N_3$  ( $n = 3$ ) were synthesized from the nominal stoichiometries  $LaN:Ru:B = 0.9:1:1$  and  $3.3:1.9:2$ , respectively.  $CaNiBN$  was also prepared using  $Ca_3N_2$ ,  $Ni$ ,  $B$ , and  $BN$  powders as starting materials. The dense sintered pellets prepared under high pressure were stable enough under an ambient atmosphere to allow characterization, unlike previously reported samples.<sup>3,8</sup>

Each sample was characterized by powder X-ray diffraction (XRD) (Bruker D8 Advance TXS, Germany) to measure the phase purity and lattice parameters. The lattice parameters were determined from the XRD data by Le Bail fitting with the software JANA2006.<sup>9</sup> Electrical resistivity ( $\rho$ ) measurements down to 1.8 K were carried out with a standard four-point-probe method using a Quantum Design Physical Property Measurement System. The magnetic susceptibility ( $\chi$ ) was measured in both zero-field-cooled (ZFC) and field-cooled (FC) modes down to 1.8 K using a Quantum Design superconducting quantum interference device magnetometer. Density functional theory (DFT) calculations to examine the electronic structure were performed using the generalized-gradient-approximation Perdew–Burke–Ernzerhof functional<sup>10</sup> in the Cambridge Serial Total Energy Package (CASTEP) code.<sup>11</sup> Density of states (DOS) calculations were based on the relaxed structures.

As shown in Figures S1 and S2 in the SI, the XRD patterns for the  $n = 2$  and 3 phases could be readily indexed with the tetragonal space groups  $P4/nmm$  and  $I4/mmm$ , which are expected for  $LuNiBC$ -type and  $La_3Ni_2B_2N_3$ -type compounds, respectively. Here  $LaT_MBN$  ( $T_M = Ru, Rh, Ir, Pt$ ) and  $La_3Ru_2B_2N_3$  were newly found phases, which are denoted by closed circles in Table S1. The lattice parameters for the materials are shown in Table S1. For  $CaNiBN$ , the lattice parameters are  $a = 3.5359(1)$  Å and  $c = 7.6394(5)$  Å. The size of the  $T_M$  square net ( $=a/\sqrt{2}$ ) is comparable to those of the reported corresponding  $T_{M2}B_2$ -based boronitrides and -carbides.<sup>2,3,8,12</sup> Strong  $T_M$ – $T_M$  bonding is expected to be present

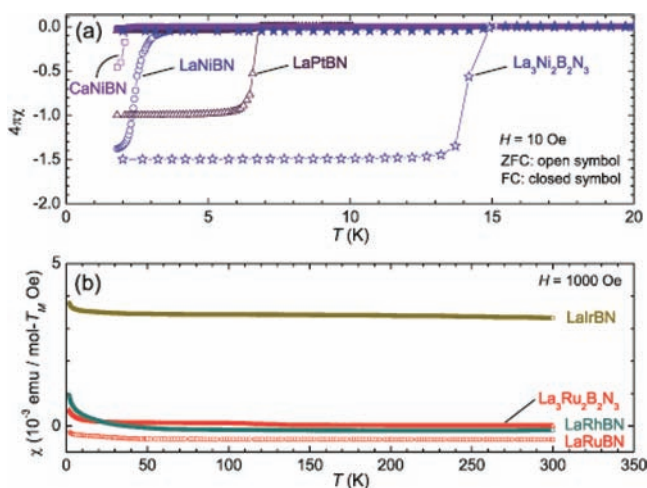
in  $(LaN)_n(T_{M2}B_2)$  ( $n = 2, 3$ ). The  $n = 2$  phase of  $LaT_MBN$  is obtained for various  $T_M$ , especially for 4d and 5d  $T_M$ , rather than the  $n = 3$  phase of  $La_3T_{M2}B_2N_3$ , which is obtained only for  $Ni$ ,  $Co$ , and  $Ru$ . Interestingly, the obtained  $T_M$  in  $LaT_MBN$  is very similar to that in  $RT_{M2}B_2C$ , despite the doping effect.

Figure 2a,b shows resistivity–temperature ( $\rho$ – $T$ ) curves for the  $n = 2$  and 3 phases, respectively. Superconductivity was



**Figure 2.** Dependence of electrical resistivity ( $\rho$ ) on temperature ( $T$ ) under zero magnetic field for the (a)  $n = 2$  and (b)  $n = 3$  phases. The inset in (a) shows an enlargement of the low-temperature region ( $T \leq 10$  K) for the  $n = 2$  phases.

observed for the  $Ni$ - and  $Pt$ -based compounds, whereas other phases showed metallic  $T$  dependence down to 1.8 K. It is worth mentioning that the  $T_c$  of the resulting  $La_3Ni_2B_2N_3$  is as high as that of the almost-stoichiometric sample.<sup>7</sup> This suggests that high-quality, nearly N-stoichiometric samples were prepared using the high-pressure synthesis.  $T_c$  systematically decreased with increasing  $H$ , indicating the superconducting transition (data not shown). The superconducting properties of the  $Ni$ - and  $Pt$ -based compounds were also confirmed by magnetic susceptibility measurements (Figure 3a). Clear diamagnetic signals were displayed within the measured temperature range, corresponding well with the resistivity data. The shielding volume fraction for each phase was large, ensuring bulk superconductivity. On the other hand, the non-superconductive phases exhibited temperature-independent magnetic susceptibility (Figure 3b). The small increase at low temperature is attributed to paramagnetic impurities. The magnetic susceptibility for  $La_3Co_2B_2N_3$  is not shown in Figure 3b because of the presence of a ferromagnetic impurity in this sample.



**Figure 3.** (a)  $T$  dependence of the magnetic susceptibility ( $4\pi\chi$ ) for superconductive Ni- and Pt-based compounds measured under 10 Oe. (b)  $\chi$ - $T$  curves for non-superconductive phases measured under 1000 Oe (FC mode).

Crystal structure data for LaNiBN and CaNiBN optimized by DFT calculations are presented in the SI. The total and projected DOS for LaNiBN are shown in Figure 4a. The energy

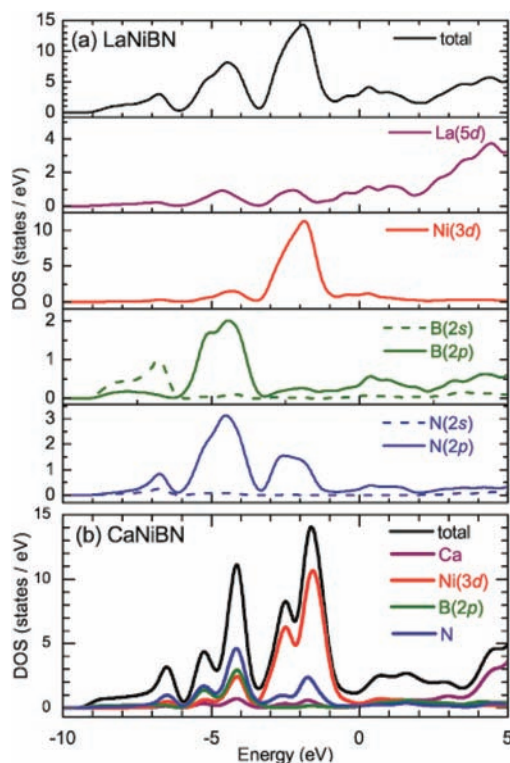


**Figure 4.** Calculated DOS of (a) LaNiBN and (b) CaNiBN, together with the projected DOS for La(5d), Ca, Ni(3d), B(2s), B(2p), N(2s), and N(2p).

levels of the relevant B orbitals are much shallower than those of N. Furthermore, the B(2s) and B(2p) levels are close in energy, unlike the case of the N(2s) and N(2p) levels. The largest DOS peak, at around  $-2$  eV with respect to  $E_F$ , is dominated by Ni(3d). The Ni(3d) contribution is clearly divided into three parts, which are ascribed to bonding, nonbonding, and antibonding states. The broad DOS around

$E_F$  is mainly dominated by the Ni(3d)-B(2p) antibonding state. It should be mentioned that an extended tail of La(5d) was also found around  $E_F$ , as observed for  $\text{La}_3\text{Ni}_2\text{B}_2\text{N}_3$ ,<sup>13</sup> which is caused by the La(5d)-N(2p) chemical bonding. For CaNiBN (Figure 4b), the contribution of Ca around  $E_F$  is less than that of La in LaNiBN, and Ni shows the largest contribution. The Fermi levels of LaNiBN and CaNiBN are located in a dip, not at the DOS peak. For the Ni(3d) nonbonding band, the energy level (to  $E_F$ ) in LaNiBN is shallower than that of CaNiBN. This effect originates from the number of electrons transferred from the counteraction (La or Ca). The main Ni(3d) bands, which are ascribed to weak antibonding states, reside well below  $E_F$  for both LaNiBN and CaNiBN.

The B-N distances in LaNiBN and CaNiBN calculated by geometry optimization are 1.45 and 1.39 Å, respectively. It should be emphasized that experimental lattice parameters for these phases deduced from the XRD patterns agreed with the calculated values within 3%. This is also true for the B-N distance in  $\text{La}_3\text{Ni}_2\text{B}_2\text{N}_3$ ,<sup>6,14</sup> which is in contrast to the previously reported experimental value for LaNiBN.<sup>15</sup> The short B-N distance indicates strong covalent bonding. In fact, similar B-N distances are found in boron nitrides [e.g., 1.45 Å for *h*-BN, 1.56 Å for *c*-BN, and 1.34 Å for  $\text{Li}_3\text{BN}_2$ , which contains a double-bonded  $(\text{N}=\text{B}=\text{N})^{3-}$  unit<sup>16</sup>]. In addition, the C-C distance in an isoelectric  $\text{C}_2$  molecular ion varies depending on the bonding state: 1.20 Å for  $(\text{C}\equiv\text{C})^{2-}$ , 1.34 Å for  $(\text{C}=\text{C})^{4-}$ , and 1.54 Å for  $(\text{C}-\text{C})^{6-}$ .<sup>16</sup> On the basis of these experimental values, it is found that the B-N distance of 1.45 Å in LaNiBN is comparable to the intermediate position between the single- and double-bonding states of the  $\text{C}_2$  dimer. Therefore, we may presume a valence state of  $(\text{BN})^{x-}$  ( $x \approx 5$ ) in LaNiBN. This estimate is consistent with the value assumed considering approximate oxidation states of +3 for La and +2 for Ni.

For the La-N distance, the DFT-calculated average value for LaNiBN is 2.66 Å, which is close to that of RS-type semimetallic LaN. This result indicates that the valence state of the LaN layer in LaNiBN may be described approximately as  $\text{La}^{(3-\delta)+}\text{N}^{(3-\delta)-}$ , even though the formal charge of the N ion is reduced because of the formation of a linear (BN) unit. Accordingly, LaNiBN is expected to exhibit 3D electronic structure.

An isolated N ion was found for the  $n \geq 3$  phases of  $(\text{RN})_n(\text{Ni}_2\text{B}_2)$ . This isolated N ion (described as N1 in Figure 1) appears to have an ionic nature because it coordinates only with R (as RS-type LaN) and never with B. Therefore, by focusing on the two chemically different N ions (N1 and N2 in Figure 1), the homologous series  $(\text{RN})_n(\text{Ni}_2\text{B}_2)$  ( $n \geq 2$ ) can be described as  $(\text{RN})_{l-2}(\text{RNiBN})_2$  ( $l \geq 2$ ). It is worth mentioning that RS-type RN is semiconducting for Sc, which is small in size, whereas it is semimetallic for lanthanides with extended 5d orbitals because of the direct  $R(5d_{xy})-R(5d_{xy})$  interaction between neighboring  $\text{RN}_6$  octahedra. As a result, the  $(\text{RN})_{l-2}$  layer in  $(\text{RN})_{l-2}(\text{RNiBN})_2$  ( $l \geq 3$ ) with extended 5d orbitals would not be expected to be a “blocking” layer and should allow a 3D metallic electronic structure, in contrast to the 2D electronic structure found in high- $T_c$  superconductors.

Superconductivity was found in LaNiBN, CaNiBN, and LaPtBN. The former two phases have been reported as non-superconductors above 4.2 K to date.<sup>3,8</sup> We consider that improvement of the sample preparation procedure plays a significant role in the emergence of superconductivity in these



materials, as  $T_c$  varies by a few kelvins depending on the sample quality, as demonstrated for  $\text{La}_3\text{Ni}_2\text{B}_2\text{N}_3$ .<sup>6,7</sup> It should be emphasized here that all of the  $\text{Ni}_2\text{B}_2$ -based compounds examined exhibit superconductivity, although their  $T_c$  values depend on the structure and constituents in the RS-type layers. It should be noted that  $E_F$  falls on the  $\text{Ni}(3d)\text{--B}(2p)$  antibonding state for all of the  $\text{Ni}_2\text{B}_2$ -based superconductors, while the main  $\text{Ni}(3d)$  band resides well below  $E_F$ . The DOS of  $\text{LaNiBN}$  and  $\text{CaNiBN}$  ( $n = 2$ ) appears at the lower tail of the DOS peak, which is consistent with the isostructural borocarbide  $\text{LuNiBC}$ . In contrast,  $E_F$  is located around the DOS peak and  $T_c \geq 15$  K for  $\text{LuNi}_2\text{B}_2\text{C}$  ( $n = 1$ ) and  $\text{La}_3\text{Ni}_2\text{B}_2\text{N}_3$  ( $n = 3$ ). Therefore, the  $T_c$  values of the  $n = 2$  boronitrides and borocarbides are similar. The above discussion is also valid for  $\text{LaPtBN}$  as well as  $\text{RT}_{M_2}\text{B}_2\text{C}$  ( $T_M = \text{Ni, Pt}$ ).<sup>4,17</sup>

When the number of d electrons was decreased by substituting Co, Rh, Ir, or Ru for Ni or Pt,  $E_F$  shifted to lower energy, and superconductivity did not appear. These observations agree with the absence of superconductivity in the  $n = 1$  borocarbides of  $\text{RT}_{M_2}\text{B}_2\text{C}$  ( $T_M = \text{Co, Rh, Ir}$ ),<sup>12</sup> suggesting common characteristics in the  $(\text{RX})_n(\text{T}_{M_2}\text{B}_2)$  series. The non-superconductive  $\text{T}_{M_2}\text{B}_2$ -based boronitrides and -carbides are Pauli paramagnetic not only for 4d and 5d  $T_M$  compounds but also for 3d  $T_M$  compounds. This is because of the shallow  $\text{B}(2p)$  orbital compared with  $\text{Pn}(p)$  level found in the relevant  $\text{ThCr}_2\text{Si}_2$ -type pnictides. Strong  $T_M(3d)\text{--B}(2p)$  covalent bonding causes a broad band, which enhances the itinerant nature of the electrons and suppresses the long-range magnetic ordering.

To summarize, we successfully synthesized the layered  $(\text{LaN})_n(\text{T}_{M_2}\text{B}_2)$  ( $n = 2, 3$ ) series by solid-state reactions in a closed system under high pressure. Bulk superconductivity was observed for the Ni- and Pt-based compounds, in which  $E_F$  is located in the band primarily composed of the  $T_M(d)\text{--B}(2p)$  antibonding state and the  $T_M(d)$  band lies well below  $E_F$ . Covalent bonding of the (BN) unit was considered to fall between the single- and double-bonding states in  $\text{LaNiBN}$ . DFT calculations indicated that  $\text{LaNiBN}$  is 3D-metallic, and the intermediate layers between neighboring  $\text{Ni}_2\text{B}_2$  layers are also metallic in  $(\text{LaN})_n(\text{Ni}_2\text{B}_2)$ . Other non-superconductive compounds exhibit Pauli paramagnetic behavior due to the strong  $T_M(d)\text{--B}(2p)$  covalent bonding, which causes the highly itinerant nature of electrons to overcome magnetic ordering interactions.

## ■ ASSOCIATED CONTENT

### 📄 Supporting Information

List of examined  $T_M$ , XRD patterns, and DFT-calculated crystallographic data (CIF). This material is available free of charge via the Internet at <http://pubs.acs.org>.

## ■ AUTHOR INFORMATION

### Corresponding Author

hosono@mssl.titech.ac.jp

### Notes

The authors declare no competing financial interest.

## ■ ACKNOWLEDGMENTS

This work was supported by the Funding Program for World-Leading Innovative R&D on Science and Technology (FIRST), Japan.

## ■ REFERENCES

- (1) (a) Kamihara, Y.; Watanabe, T.; Hirano, M.; Hosono, H. *J. Am. Chem. Soc.* **2008**, *130*, 3296. (b) Ren, Z.; Lu, W.; Yang, J.; Yi, W.; Shen, X.; Li, Z.; Che, G.; Dong, X.; Sun, L.; Zhou, F.; Zhou, Z. *Chin. Phys. Lett.* **2008**, *25*, 2215.
- (2) (a) Cava, R. J.; Takagi, H.; Zandbergen, H. W.; Krajewski, J. J.; Peck, W. F. Jr.; Siegrist, T.; Batlogg, B.; van Dover, R. B.; Felder, R. J.; Mizuhashi, K.; Lee, J. O.; Eisaki, H.; Uchida, S. *Nature* **1994**, *367*, 252. (b) Eisaki, H.; Takagi, H.; Cava, R. J.; Batlogg, B.; Krajewski, J. J.; Peck, W. F. Jr.; Mizuhashi, K.; Lee, J. O.; Uchida, S. *Phys. Rev. B* **1994**, *50*, 647.
- (3) Cava, R. J.; Zandbergen, H. W.; Batlogg, B.; Eisaki, H.; Takagi, H.; Krajewski, J. J.; Peck, W. F. Jr.; Gyorgy, E. M.; Uchida, S. *Nature* **1994**, *372*, 245.
- (4) (a) Pickett, W. E.; Singh, D. J. *Phys. Rev. Lett.* **1994**, *72*, 3702. (b) Mattheiss, L. F. *Phys. Rev. B* **1994**, *49*, 13279.
- (5) Singh, D. J. *Phys. Rev. B* **2008**, *78*, No. 094511.
- (6) (a) Wideman, T.; Cava, R. J.; Sneddon, L. G. *Chem. Mater.* **1996**, *8*, 2215. (b) Blaschkowski, B.; Meyer, H.-J. *Z. Anorg. Allg. Chem.* **2002**, *629*, 129.
- (7) Ali, T.; Rupperecht, C.; Khan, R. T.; Bauer, E.; Hilscher, G.; Michor, H. *J. Phys.: Conf. Ser.* **2010**, *200*, 012004.
- (8) Blaschkowski, B.; Meyer, H.-J. *Z. Anorg. Allg. Chem.* **2002**, *628*, 1249.
- (9) Petricek, V.; Dusek, M.; Palatinus, L. *JANA2006*; Institute of Physics: Praha, Czech Republic, 2006.
- (10) Perdew, J. P.; Burke, K.; Ernzerhof, M. *Phys. Rev. Lett.* **1996**, *77*, 3865. Perdew, J. P.; Burke, K.; Ernzerhof, M. *Phys. Rev. Lett.* **1997**, *78*, 1396.
- (11) Clark, S. J.; Segall, M. D.; Pickard, C. J.; Hasnip, P. J.; Probert, M. J.; Refson, K.; Payne, M. C. *Z. Kristallogr.* **2005**, *220*, 567.
- (12) (a) Cava, R. J.; Siegrist, T.; Batlogg, B.; Takagi, H.; Eisaki, H.; Carter, S. A.; Krajewski, J. J.; Peck, W. F. Jr. *Phys. Rev. B* **1994**, *50*, 12966. (b) Kadowaki, K.; Takeya, H.; Hirata, K.; Mochiku, T. *Physica B* **1995**, *206–207*, 555. (c) Hsu, Y. Y.; Chiang, H. C.; Ku, H. C. *J. Appl. Phys.* **1998**, *83*, 6789.
- (13) Singh, D. J.; Pickett, W. E. *Phys. Rev. B* **1995**, *51*, 8668.
- (14) Singh, D. J.; Pickett, W. E. *Nature* **1995**, *374*, 682.
- (15) Zandbergen, H. W.; Jansen, J.; Cava, R. J.; Krajewski, J. J.; Peck, W. F. Jr. *Nature* **1994**, *372*, 759.
- (16) (a) Yamane, H.; Kikkawa, S.; Horiuchi, H.; Koizumi, M. *J. Solid State Chem.* **1986**, *65*, 6. (b) Wells, A. F. *Structural Inorganic Chemistry*, 5th ed.; Clarendon Press: Oxford, U.K., 1986. (c) Gerss, M. H.; Jeitschko, W.; Boonk, L.; Nientiedt, J.; Grobe, J.; Mörsen, E.; Leson, A. *J. Solid State Chem.* **1987**, *70*, 19.
- (17) Singh, D. J. *Phys. Rev. B* **1994**, *50*, 6486.